Nonlinear Biot waves in porous media with application to unconsolidated granular media

Olivier Dazel and Vincent Tournat[a)]
LAUM, CNRS, Université du Maine, Avenue Olivier Messiaen, 72085 Le Mans, France

(Received 3 November 2008; revised 15 October 2009; accepted 24 November 2009)

The nonlinear propagation through porous media is investigated in the framework of Biot theory. For illustration, and considering the current interest for the determination of the elastic properties of granular media, the case of nonlinear propagation in "model" granular media (disordered packings of noncohesive elastic beads of the same size embedded in a visco-thermal fluid) is considered. The solutions of linear Biot waves are first obtained, considering the appropriate geometrical and physical parameters of the medium. Then, making use of the method of successive approximations of nonlinear acoustics, the solutions for the second harmonic Biot waves are derived by considering a quadratic nonlinearity in the solid frame constitutive law (which takes its origin from the high nonlinearity of contacts between grains). The propagation in a semi-infinite medium with velocity dispersion, frequency dependent dissipation, and nonlinearity is first analyzed. The case of a granular medium slab with rigid boundaries, often considered in experiments, is then presented. Finally, the importance of mode coupling between solid and fluid waves is evaluated, depending on the actual fluid, the bead diameter, or the applied static stress on the beads. The application of these results to other media supporting Biot waves (porous ceramics, polymer foams, etc.) is straightforward. © *2010 Acoustical Society of America.* [DOI: 10.1121/1.3277190]

PACS number(s): 43.25.Dc, 43.20.Jr, 43.20.Gp, 43.20.Bi [ROC] Pages: 692–702

I. INTRODUCTION

The acoustics of granular media has been widely investigated among different fields such as geophysics, underwater, or airborne acoustics (sound proofing, shock wave absorption, etc.). Recently in physics, granular materials have attracted a strong interest because they exhibit unusual behaviors.[1,2] These behaviors are sometimes comparable to glassy media, from the point of view of the aging process, for instance,[3] or regarding the prediction of the soft modes and their relation to the boson peak.[4,5] The transition from one state to another, and, in particular, the unjamming transition from a solid-like to a fluid-like phase, is intensively studied.[6] One key point for the related experimental and theoretical investigations is to obtain the elastic properties of the granular materials. Their geometrical properties being better characterized thanks to several existing methods such as x-ray tomography, γ-ray transmission, and iso-index optical imaging, for instance.[3] In this context, acoustic waves are the only one able to probe accurately the elastic properties in the bulk of three-dimensional media and should contribute to the experimental characterization of the aforementioned processes.

Frequently, due to the complexity in behaviors and structures of granular media (sand, sediments, etc.) and due to the subsequent lack of realistic modeling, it is of interest to study ''model'' granular media such as disordered packings of noncohesive spherical beads of the same size. In this type of model media, there exists a characteristic scale, the diameter d of the beads, and one can use a constitutive law at the level of the contacts such as the Hertz or the Hertz–Mindlin contact laws.[7,8] The intrinsic nonlinearities ensure a parameter of quadratic nonlinearity for these media 100–1000 times larger than in homogeneous fluids and solids.[9] As a consequence, various nonlinear acoustic effects have been observed for moderate excitation amplitudes.[10–16] They are able to give complementary information on the elastic properties of model granular media. In particular, nonlinear waves exhibit a preferential sensitivity to the most weakly stressed contacts of the granular packing[14,16] (a distribution of contact stresses exists due to the disordered structure of the granular packing[17]) compared to the linear waves.

The results on the elastic wave propagation in the solid frame of model granular media contain several features, such as a dependence of longitudinal and shear wave velocities on the applied static pressure,[18,19,14] a frequency dependent attenuation, a velocity dispersion, multiple scattering effects at wavelengths of the order of the bead diameter,[19] memory effects,[20] hysteresis,[10] response fluctuations,[4] dynamic dilatancy,[14] and nonlinearities.

Most of the studies on wave propagation through model granular media either consider the propagation through the solid network, neglecting the saturating fluid, or consider the propagation through the fluid phase saturating the rigid bead packing, which is assumed to be motionless.

For waves propagating in the fluid saturating the bead packing, the equivalent fluid model (i.e., the solid is motionless) has been successfully applied to the case of long-wavelength propagation in air saturating glass beads, for instance,[21–23] and provides the evaluation of useful parameters for the present work. Theoretical investigations on air-saturated granular media in the frame of the equivalent fluid model have also been performed.[24,22,25] Nonlinear effects

[a)]Author to whom correspondence should be addressed. Electronic mail: vincent.tournat@univ-lemans.fr

have been investigated in this equivalent fluid model approximation in the case of intense sound waves.[26] For shorter wavelengths, becoming of the order of the bead diameter, scattering occurs and its modeling for such close scatterers is a hard task even if the geometry is well-known.[27] In water, owing to the lower acoustic energy dissipation than in air, several pioneering experiments have been carried out on the acoustic energy diffusion process and showed that most of the energy transports through water and that the associated waves are multiply scattered by the glass beads.[28]

There are only few experiments where both waves in the fluid and in the bead structure have been shown to play a role and to couple. In Ref. 29, the nonlinear self-demodulation process has been experimentally observed with a transmission toward the air of the frequency component nonlinearly generated inside the solid frame.

The aim of this article is to use the Biot theory,[30,31] generally applied to linear acoustics, to model the nonlinear propagation in porous media, with an application to granular media.

Biot theory describes the deformation of a porous deformable elastic solid in which the nonsolid part is saturated by a compressible fluid. Even if Biot theory is not able to model the behavior of every type of porous materials (porous rocks, etc.), it has been successfully applied to a wide range of materials[32,33] using homogenization techniques[34,35] or volume averaging methods.[36,37] The application of Biot theory to sound absorbing materials takes its origin in the beginning of 1980s. For acoustical materials, the saturating fluid is air. The description of the viscous and thermal properties of air saturating a porous immobile solid has been a wide research topic and many models have been published.[38–41,36] These models consist in introducing a frequency dependent complex density (respectively, compressibility) to take into account viscous (respectively, thermal) effects. Extensive details on these aspects can be found in Refs. 38, 42, and 43.

In this article, an extension of the Biot theory is first presented to describe the nonlinear acoustic propagation in a nonlinear porous solid, where the motion of the solid and fluid phases with viscous and thermal effects is considered. Inertial and elastic couplings between both constituents are considered. This work is mainly based on two references in the literature[44,45] about nonlinear wave propagation in porous media. The originality of the present study is first to propose a new formulation to describe the nonlinear Biot wave propagation, which allows for significant simplifications of the existing expressions without any additional assumptions, second to take into account the viscous and thermal effects through Johnson–Allard's models, and finally, to apply the theory to unconsolidated granular media. In the case of interest, the parameters of the Biot theory corresponding to "model" granular media are used, but the theoretical results could be applied to other media supporting Biot waves, such as sediments, porous ceramics, polymer foams, and trabecular bone,[46] possibly with other saturating fluids. After the presentation of the theory, we analyze the effect of second harmonic generation in a one-dimensional geometry for a semi-infinite medium and for a slab configuration. We describe the influence of some parameters on the mode coupling and on the nonlinear effects (such as the bead diameter, for instance, or parameters of the solid frame and of the saturating fluid). This allows to evaluate the importance of the often neglected effects of coupling in the linear and nonlinear acoustic experiments on model granular media.

II. BIOT THEORY WITH QUADRATIC NONLINEARITY

A. Nonlinear Biot equations in $\{\mathbf{u}^s,\mathbf{u}^W\}$ formulation

Biot theory[31] is able to model the acoustic propagation through homogenized porous media using six fields, which can be, depending on the chosen formulation, the three displacements of each homogenized phase ($\mathbf{u}^s$ and $\mathbf{u}^f$, respectively, for the solid and fluid displacements) or any free linear combination[30,47] of these two fields. As the 1956 (Ref. 31) formulation was not valid for porous material with an inhomogeneous porosity ϕ, Biot[30] derived a second formulation in which the considered fields are the solid displacement $\mathbf{u}^s$ and the relative flow $\mathbf{w}=\phi(\mathbf{u}^f-\mathbf{u}^s)$. Recently, Dazel *et al.*[47] published a strain decoupled formulation (equivalent to 1962 formulation), which simplifies the Biot formalism without additional assumptions. One goal of this article is to show that similar simplifications can also be obtained for nonlinear porous materials. The fields involved in the present formulation are the solid displacement $\mathbf{u}^s$ and the strain decoupled displacement field $\mathbf{u}^W=\mathbf{u}^t+(\alpha-1)\mathbf{u}^s$, where $\alpha=1-K_s/K_r$ (K_r is the bulk modulus of the bead matter, glass for the example in Sec. II B, and K_s is the bulk modulus of the porous solid in vacuum) and where $\mathbf{u}^t=(1-\phi)\mathbf{u}^s+\phi\mathbf{u}^f$ is the total displacement of the porous medium.

In $\{\mathbf{u}^s,\mathbf{u}^W\}$ formulation, the equations of motion at cyclic frequency ω read as[47]

$$\sigma^s_{ij,j}(\mathbf{u}^s)=-\omega^2\tilde{\rho}_s\mathbf{u}^s-\omega^2\tilde{\rho}_{\mathrm{eq}}\tilde{\gamma}\mathbf{u}^W, \tag{1a}$$

$$-\boldsymbol{\nabla}p=-\omega^2\tilde{\rho}_{\mathrm{eq}}\tilde{\gamma}\mathbf{u}^s-\omega^2\tilde{\rho}_{\mathrm{eq}}\mathbf{u}^W, \tag{1b}$$

where $\tilde{\rho}_{\mathrm{eq}}$ and $\tilde{\rho}_s$ are equivalent densities and $\tilde{\gamma}$ is a coupling coefficient. The tilde symbol "~" is associated with frequency dependent coefficients at frequency ω, $\boldsymbol{\nabla}$ denotes the partial derivative nabla operator, p corresponds to the interstitial pressure, and σ^s_{ij} is the *in-vacuo* stress tensor of the solid phase. For a linear constitutive law, it has been shown that σ^s_{ij} only depends on $\mathbf{u}^s$ and that p only depends on $\mathbf{u}^W$,[47]

$$\sigma^s_{ij}=2\mu\varepsilon_{ij}+\lambda\varepsilon\delta_{ij},\quad p=-M\xi, \tag{2}$$

where λ and μ are the Lamé coefficients of the solid, M is the equivalent compressibility of the equivalent fluid model, ε_{ij} is the strain tensor of the solid phase, δ_{ij} is the Kronecker tensor, $\varepsilon=\boldsymbol{\nabla}\cdot\mathbf{u}^s$, and $\xi=\boldsymbol{\nabla}\cdot\mathbf{u}^W$. In the two other formulations[30,31] the conjugated stresses depend on both displacement fields. Moreover, σ^s_{ij} is related to the total stress tensor σ^t_{ij} by the following relation:

$$\sigma^s_{ij}=\sigma^t_{ij}+\alpha p\delta_{ij}. \tag{3}$$

Stress-strain relations (2) are modified in the case of a nonlinear porous material. As mentioned in Sec. I, the nonlinearity of granular media mainly comes from the contacts between beads and is several orders of magnitude higher than

in homogeneous solids and fluids.[9] Even at moderate excitation amplitudes, nonlinear effects have been observed.[10–16] As a consequence, in the present case, we neglect Forchheimer's nonlinearity, which has been shown to play a role in some air-saturated porous media at high acoustic levels in the context of a rigid solid frame (equivalent fluid approximation).[26] A way to consider nonlinear terms in the constitutive laws has been described by Biot[44] and Donskoy *et al.*[45] and consists in introducing a nonlinear potential H defined by

$$H = D\left(\frac{\bar{I}_1^3}{3} - \bar{I}_1\bar{I}_2 + \bar{I}_3\right) + F(\bar{I}_1\bar{I}_2 - 3\bar{I}_3) + G\bar{I}_3 \tag{4}$$

where the $\bar{I}_i$ are the strain invariants associated with the modified strain[45] $\bar{\varepsilon}_{ij}$ defined by

$$\bar{\varepsilon}_{ij} = \varepsilon_{ij} + p\theta\delta_{ij}, \tag{5}$$

where $\theta = K_r/3$ is the fluid compliance coefficient. The strain invariants are

$$\bar{I}_1 = \mathrm{tr}(\bar{\varepsilon}_{ij}), \quad \bar{I}_2 = \bar{\varepsilon}_{11}\bar{\varepsilon}_{22} + \bar{\varepsilon}_{11}\bar{\varepsilon}_{33} + \bar{\varepsilon}_{22}\bar{\varepsilon}_{33} - \bar{\varepsilon}_{12}\bar{\varepsilon}_{21} - \bar{\varepsilon}_{13}\bar{\varepsilon}_{31} - \bar{\varepsilon}_{23}\bar{\varepsilon}_{32}, \quad \bar{I}_3 = \det(\bar{\varepsilon}_{ij}). \tag{6}$$

The nonlinear constitutive laws with the nonlinear potential H are then written [Eq. (2)] as

$$\sigma_{ij}^s = 2\mu\varepsilon_{ij} + \lambda\varepsilon\delta_{ij} + \partial_{\bar{\varepsilon}_{ij}}H, \tag{7a}$$

$$p = -M\xi + M\theta\delta_{ij}\partial_{\bar{\varepsilon}_{ij}}H. \tag{7b}$$

These two equations [Eqs. (7a) and (7b)] correspond to relations (12) in Ref. 45. Equation (7b) is equivalent to the second relation (12) of Ref. 45 but one can notice that relation (7b) has the advantage of involving in its linear part only the divergence of $\mathbf{u}^W$ instead of the mixture law $\boldsymbol{\nabla}(\mathbf{w}+\alpha\mathbf{u}^s)$. The use of the *in-vacuo* stress instead of the total stress tensor of the porous medium implies that the pressure p does not appear in Eq. (7a) as it is the case for the first relation (12) in Ref. 45 for the total stress tensor. The problem of elimination of the pressure from σ^t was mentioned in Ref. 45 and does not stand in our formulation of the poroelasticity equations. It is an advantage of the present formulation.

The nonlinear contributions of H to the *in-vacuo* stress and pressure can be expanded and read as

$$\partial_{\bar{\varepsilon}_{ij}}H = F\bar{I}_1^2\delta_{ij} + (F-D)(\delta_{ij}\bar{I}_2 - \bar{I}_1\bar{\varepsilon}_{ij}) + (G+D-3F)\mathrm{cof}(\bar{\varepsilon}_{ij}), \tag{8a}$$

$$\delta_{ij}\partial_{\bar{\varepsilon}_{ij}}H = 3F\bar{I}_1^2 + (F-D)(3\bar{I}_2 - \bar{I}_1^2) + (G+D-3F)\bar{I}_2 = P\bar{I}_1^2 + (G-2D)\bar{I}_2, \tag{8b}$$

with $P=D+2F$ and $\mathrm{cof}(\bar{\varepsilon}_{ij})$ corresponds to the matrix of cofactors.

B. One-dimensional problem

Only one-dimensional problems are considered in the following, which implies simplifications that are now detailed for the nonlinear terms. The displacement fields are along the x direction, and all the fields of the problem only depend on x. The space derivation with respect to x is denoted by subscript $_{,x}$ ($_{,xx}$ for the second derivative). Hence x corresponds to the direction 1 of Sec. II A and directions 2 and 3 are not considered. In this case, the strain invariants read as

$$\bar{I}_1 = u_{,x}^s + 3\theta p, \quad \bar{I}_2 = (2u_{,x}^s + 3\theta p)\theta p, \quad \bar{I}_3 = (u_{,x}^s + \theta p)\theta^2 p^2, \tag{9}$$

and the nonlinear contributions to the stress are

$$\partial_{\bar{\varepsilon}_{ij}}H = D(u_{,x}^s)^2 + 2P(\theta p u_{,x}^s) + K(\theta p)^2, \tag{10a}$$

$$\delta_{ij}\partial_{\bar{\varepsilon}_{ij}}H = P(u_x^s)^2 + 2K\theta p u_x^s + 3K(\theta p)^2, \tag{10b}$$

with $K=D+6F+G$. In the following, the method of successive approximation is used, and the forces corresponding to the nonlinear terms contain only the linear solutions previously computed (and denoted with an l index) u_l^s and u_l^W. Consequently, the pressure p_l in the nonlinear terms is defined by relation (2) and $p_l = -Mu_{l,x}^W$. The forces associated with the nonlinear potential are then written as

$$\partial_{\bar{\varepsilon}_{ij}}H_{l,x} = 2Du_{l,x}^s u_{l,xx}^s - 2MP\theta(u_{l,xx}^W u_{l,x}^s + u_{l,x}^W u_{l,xx}^s) + 2KM^2\theta^2 u_{l,x}^W u_{W,xx}^t, \tag{11a}$$

$$\delta_{ij}\partial_{\bar{\varepsilon}_{ij}}H_{l,x} = 2Pu_{l,x}^s u_{l,xx}^s - 2MK\theta(u_{l,xx}^W u_{l,x}^s + u_{l,x}^W u_{l,xx}^s) + 6KM^2\theta^2 u_{l,x}^W u_{l,xx}^W. \tag{11b}$$

These two last equations are compared to Eqs. (20) and (21) of Ref. 45 obtained with $\{\mathbf{u}^s, \mathbf{w}\}$ formulation. In comparison, it is important to note the drastic simplifications of the nonlinear forces in Eq. (11) obtained using our formulation in $\{\mathbf{u}^s, \mathbf{u}^W\}$ without loss of generality.

C. Simplifications associated with the stiffness ratio between the solid frame and the frame material

Additional simplifications can be made in the case of granular media taken here as an illustration, and for other porous media supporting Biot waves as long as the following conditions on compressibility are fulfilled. The bead material is much stiffer than the contacts between beads (and consequently the solid frame),[7] which leads to the following strong inequalities: $K_r \gg K_s$ and $K_r \gg K_f$. Consequently, $\alpha \approx 1$, which leads to $u^W = u^t$. Also $\theta M \approx K_f/3\phi K_r \ll 1$. Hence, the only remaining nonlinear term in Eq. (11a) is the one containing $u_{l,x}^s u_{l,xx}^s$ and the constitutive law [Eq. (7b)] can be approximated by its linear part.

For model granular media, the quadratic elastic nonlinearity is a reasonably good first approximation[11,14,15] as for other porous media, in order to explain the harmonic generation process, at least for some moderate range of excitation amplitude.[13,14] Consequently, we keep this type of nonlinearity as the starting point of the present study. The value of the parameter of quadratic nonlinearity has been measured to be several orders of magnitude higher than in homogeneous

fluid or solids,[9,12] but can vary over a wide range depending on the external conditions of static stress or on the particular bead arrangement, for instance.[48]

With the previous assumptions, the one-dimensional equations of motion for a model granular porous medium read as

$$\lambda_c u^s_{,xx} + 2Du^s_{,x}u^s_{,xx} = -\omega^2\tilde{\rho}_s u^s - \omega^2\tilde{\gamma}\tilde{\rho}_{\mathrm{eq}}u^t, \tag{12a}$$

$$Mu^t_{,xx} = -\omega^2\tilde{\gamma}\tilde{\rho}_{\mathrm{eq}}u^s - \omega^2\tilde{\rho}_{\mathrm{eq}}u^t, \tag{12b}$$

where $\lambda_c=\lambda+2\mu$. In the following, the value $2D=100\lambda_c$ is taken everywhere. Considering this value for the parameter of quadratic nonlinearity, the expansion of the stress-strain relationship up to the quadratic term is valid if $|u^s_{,x}| \ll 1/50$. In this manuscript, dispersive viscous and thermal effects of the fluid are taken into account based on Johnson *et al.*[40] and Champoux–Allard[39] models. It is not the case in Refs. 44 and 45. Details on these models can be found in Appendix B.

D. Case of the pure elastic solid

It is instructive to consider the pure elastic solid case, which corresponds to the propagation of a single mode in the solid frame. This allows to compare our results with other studies of acoustic propagation in granular media, which neglect the influence of the saturating fluid. Note that inertial coupling effects with the fluid are taken into account but not the thermal effects, unlike the so-called *in-vacuo* stress, which neglects completely the saturating fluid. This case is called "elastic" in the following (unlike poroelastic for the Biot modes), and the comparison of the elastic and poroelastic solutions should reveal the influence of the saturating fluid. The unknown elastic displacement field is denoted by u^e and the motion equation [Eq. (12)] becomes

$$\lambda_c u^s_{,xx} + 2Du^e_{,x}u^e_{,xx} = -\omega^2\tilde{\rho}u^e. \tag{13}$$

The method of successive approximations is also applied for this problem and is detailed in Appendix A 2.

III. RESOLUTION OF THE PROBLEM

The method of successive approximations is used to solve the problem of second harmonic generation at the leading order of nonlinearity.[49,50] It is equivalent to solving a so-called "weak nonlinear" problem, where the nonlinear acoustic effects are quadratic and the nonlinear interactions only take place once for the fundamental wave (or primary radiated wave). This gives the limit of applicability for this quadratic approximation: the primary wave amplitude should be weak enough so that the nonlinearly generated components (such as the second harmonic wave) exhibit negligible nonlinear effects themselves.

The first step of this method is to find the solution $\{u^s_l, u^t_l\}$ of the linear problem at frequency ω for which the nonlinearity is omitted. The second step is to write the problem [Eq. (12)] at frequency 2ω and to substitute the solution of the linear problem at frequency ω in the nonlinear term $2Du^s_{,x}u^s_{,xx}$ of Eq. (12). This term then acts as a source term for the second harmonic wave. A second linear problem, at frequency 2ω, is solved. Simple mathematics shows that the solution of this problem is the superposition of the particular and the general solutions. It is important to note that in this weakly nonlinear quadratic approximation, no nonlinear effect on wave speed (in average over a wave period) and attenuation occur.[49]

A. General form of the solutions

It is straightforward by the methods of characteristics[38,31] to show that the solution of the linear problem at frequency ω is a superposition of two compressional waves, where the solid and total displacements read as

$$u^s_l = (u_1 e^{-jk_1 x} + u_2 e^{-jk_2 x} + u'_1 e^{jk_1 x} + u'_2 e^{jk_2 x})e^{j\omega t}, \tag{14a}$$

$$u^t_l = (\mu_1 u_1 e^{-jk_1 x} + \mu_2 u_2 e^{-jk_2 x} + \mu_1 u'_1 e^{jk_1 x} + \mu_2 u'_2 e^{jk_2 x})e^{j\omega t}, \tag{14b}$$

where u_1, u_2, u'_1, and u'_2 are coefficients determined by the boundary conditions of the problem, and k_1 and k_2 are the wave numbers of the two compressional waves. For each one of these modes, μ_i is the ratio of the total displacement amplitude over the solid one. Their expressions are given at the end of Appendix B.

The particular solution of the problem at 2ω can be written in the following forms:

$$u^s_p = \alpha_0 + \left(\sum_{i=1}^{4} \alpha_i e^{-2jk_i x} + \alpha'_i e^{2jk_i x}\right)e^{2j\omega t}, \tag{15}$$

$$u^t_p = \beta_0 + \left(\sum_{i=1}^{4} \beta_i e^{-2jk_i x} + \beta'_i e^{2jk_i x}\right)e^{2j\omega t}, \tag{16}$$

where $2k_3=k_1+k_2$, $2k_4=k_1-k_2$, and α_i and β_i are obtained through an identification method presented in Appendix A. The form of the general solution of the problem at 2ω is quite similar to the linear solution

$$u^s_g = (\gamma_1 e^{-j\ddot{k}_1 x} + \gamma_2 e^{-j\ddot{k}_2 x} + \gamma'_1 e^{j\ddot{k}_1 x} + \gamma'_2 e^{j\ddot{k}_2 x})e^{2j\omega t}, \tag{17a}$$

$$u^t_g = (\ddot{\mu}_1\gamma_1 e^{-j\ddot{k}_1 x} + \ddot{\mu}_2\gamma_2 e^{-j\ddot{k}_2 x} + \ddot{\mu}_1\gamma'_1 e^{j\ddot{k}_1 x} + \ddot{\mu}_2\gamma'_2 e^{j\ddot{k}_2 x})e^{2j\omega t}. \tag{17b}$$

The double dot symbol "¨" denotes the 2ω values of the coefficients (for example, $\ddot{k}_1$ corresponds to the wave number of the first Biot wave at cyclic frequency 2ω). The γ_i are amplitudes determined by the boundary conditions for the nonlinear solution of the problem at 2ω.

B. Case of a semi-infinite porous medium

The case of a semi-infinite porous medium is first considered. Accordingly, there is no counter-propagating wave. This imposes that the amplitudes u'_1 and u'_2 are zero. A sinusoidal displacement with amplitude u_0 and frequency ω is imposed at $x=0$ on the solid and the fluid. The associated boundary condition is consequently $u^l_s(0)=u^l_t(0)=u_0$.[38,47] Then, u_1 and u_2 are solutions of the following system:

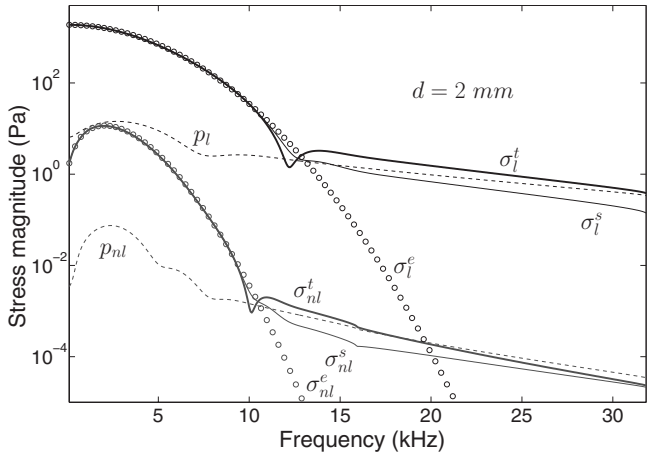

FIG. 1. Linear (at frequency ω) and nonlinear (at frequency 2ω) stress magnitudes at a distance $x=10$ cm from the excitation boundary in the semi-infinite configuration. σ^s, σ^f, σ^t, and σ^e are, respectively, the solid, fluid, total, and elastic stresses. Indices l and "nl" are, respectively, used for the linear and the nonlinear contributions. Note that the frequency axis indicates the fundamental frequency, i.e., the magnitude for the second harmonic at 2ω frequency should be read at ω. Case of air-saturated elastic beads of diameter 2 mm.

$$\begin{bmatrix} 1 & 1 \\ \mu_1 & \mu_2 \end{bmatrix} \begin{Bmatrix} u_1 \\ u_2 \end{Bmatrix} = \begin{Bmatrix} u_0 \\ u_0 \end{Bmatrix}, \tag{18}$$

which solutions read as

$$u_1 = \frac{\mu_2 - 1}{\mu_2 - \mu_1} u_0, \quad u_2 = \frac{\mu_1 - 1}{\mu_1 - \mu_2} u_0. \tag{19}$$

For the particular and general solutions of the problem at 2ω, the prime coefficients associated with the counter-propagating waves are also zero. This corresponds to consider only cumulative nonlinear effects. Local nonlinear effects, neglected in this theory, could in principle allow for the generation of counter-propagating second harmonic wave, but with a much lower efficiency. The particular solution is obtained using the method in Appendix A. The boundary conditions relative to the nonlinear displacements are the nullity of the solid and total displacements at $x=0$. Hence, γ_1 and γ_2 are solutions of

$$\begin{bmatrix} 1 & 1 \\ \ddot{\mu}_1 & \ddot{\mu}_2 \end{bmatrix} \begin{Bmatrix} \gamma_1 \\ \gamma_2 \end{Bmatrix} = - \begin{Bmatrix} \alpha_1 + \alpha_2 + \alpha_3 \\ \beta_1 + \beta_2 + \beta_3 \end{Bmatrix}, \tag{20}$$

and their expressions are

$$\gamma_1 = \frac{\ddot{\mu}_2(\alpha_1 + \alpha_2 + \alpha_3) - (\beta_1 + \beta_2 + \beta_3)}{\ddot{\mu}_1 - \ddot{\mu}_2}, \tag{21a}$$

$$\gamma_2 = \frac{-\ddot{\mu}_1(\alpha_1 + \alpha_2 + \alpha_3) + (\beta_1 + \beta_2 + \beta_3)}{\ddot{\mu}_1 - \ddot{\mu}_2}. \tag{21b}$$

In Fig. 1, the magnitude of the acoustic stress at a 10 cm distance from the source is plotted as a function of frequency. The excitation displacement at $x=0$ is imposed in the form $u=u_0 \sin(\omega t)$ with $u_0=0.001\times 2\pi/\omega$, which corresponds to an imposed strain amplitude independent of frequency and of realistic magnitude of 3×10^{-5} for a medium without dispersion. This is also close to the efficiency of wide-band ultrasonic transducers in experiments.[51] The stress in the solid frame σ^s (supported by the beads and their contacts) and the fluid pressure p both contribute to the total stress σ^t. The pure elastic stress is denoted by σ^e. Linear and nonlinear stresses, corresponding here to the contributions at frequencies ω and 2ω, respectively, are plotted separately for clarity because the linear stress is most of the time dominant over the nonlinear one for this process of second harmonic generation. The linear stresses are indexed with l while the nonlinear stresses are indexed with "nl."

For all the figures in this article, when it is not specified, the wave and medium parameters are those in Appendix B. These parameters are chosen in agreement with available experimental results[51,14,15] for weakly stressed granular packings of glass beads. The equivalent fluid parameters of the glass bead packing and their scaling laws with the bead radius are mostly taken from Ref. 21 (see Appendix B). The longitudinal wave velocity in the solid frame in the long wavelength limit is 200 m/s. It decreases with frequency as observed in sand and model granular media, and due to the absence of models of velocity dispersion in disordered three-dimensional bead packings, the dispersion law of a one-dimensional granular chain is used. The corresponding wavelength is 2 cm at 10 kHz (ten times larger than the bead diameter) and ~0.7 cm at 30 kHz. Due to the occurrence of scattering, the limit of applicability of the Biot theory is reached for the highest frequencies of the plots. However, this frequency limit of applicability can be increased if the coherent wave is considered by performing a spatial averaging of the acoustic field (over different configurations of the medium or by transducers with a sensitive surface larger than the wavelength, for instance). Scattering in this case would result in additional attenuation and velocity dispersion.

The linear elastic stress σ_l^e monotonously decreases in magnitude with increasing frequency because of the attenuation proportional to ω. Such as in a homogeneous solid or fluid with a quadratic nonlinearity and an increasing attenuation with frequency, the nonlinear stress σ_{nl}^e first increases with frequency, reaches a maximum, and then decreases. The linear solid stress σ_l^s has a different behavior than σ_l^e, showing that under the considered conditions, the coupling between the solid frame and the saturating fluid cannot be neglected here. It is possible to define a characteristic frequency f_c, from which σ_l^s deviates significantly from σ_l^e. This corresponds to a crossover between the two Biot waves. Below this frequency, the dynamics is mainly solid controlled, and above this frequency, it is fluid controlled. Around this frequency f_c, the solid and fluid waves are of comparable magnitude, and their interferences produce the notch at 13 kHz. It is important to mention that this crossover is not always characterized by a local minimum in σ_l^t, as shown in Fig. 1. The same qualitative behavior can be observed for the nonlinear stresses at frequency 2ω.

In Fig. 2, the same quantities as in Fig. 1 are plotted but as a function of distance from the excitation boundary at the fixed frequency of 10 kHz. At small distance from the source, the linear total stress σ_l^t is mainly supported by the solid and decreases exponentially with distance as does the pure elastic stress σ_l^e for the whole frequency range (a linear

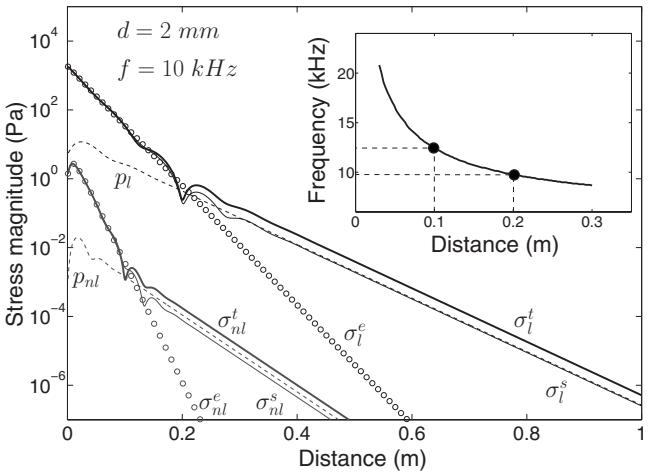

FIG. 2. Linear and nonlinear stress magnitudes as a function of distance from the source in the semi-infinite configuration. Same notations as in Fig. 1. The inset shows the relation between the excitation frequency and the propagation distance for the occurrence of the crossover between σ_l^s and p_l.

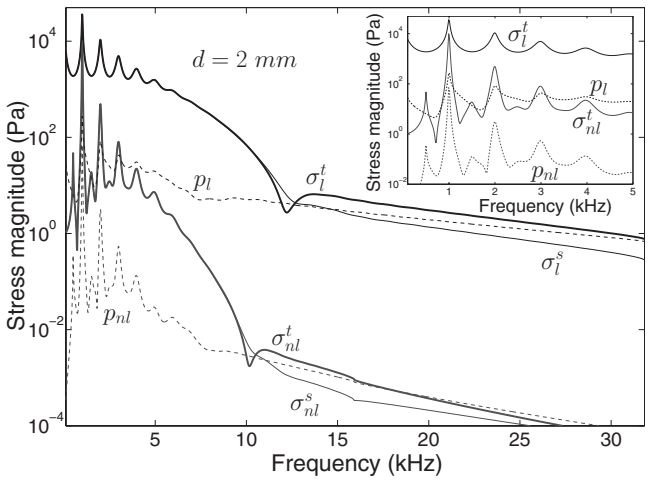

FIG. 3. Linear and nonlinear stress magnitudes at $x=0$ for a 10 cm slab configuration. Same notations and parameters as in Fig. 1. The inset shows a zoom of the low-frequency region.

decrease in the semilog plot). At a distance of approximately 20 cm from the source a crossover occurs: the fluid and solid stresses are of comparable magnitude. For longer distances, the behavior of the total stress is determined dominantly by the fluid properties as it clearly deviates from the behavior of the pure elastic stress σ_l^e. The reason of this crossover is that the solid Biot wave is more damped than the fluid wave. Consequently, for long enough distances, the acoustic energy initially injected in the solid is strongly damped, and the only remaining wave, able to propagate in the fluid, releases energy to the solid frame by coupling. The response of the system cannot be accurately predicted by a model, neglecting the solid-fluid interactions, which justifies the use of the Biot theory.

C. Harmonic generation in the slab configuration

The slab configuration consisting of an excitation boundary at $x=-d$ and a rigid boundary at $x=0$ is now investigated. The slab configuration qualitatively corresponds to the one used in some available experimental results.[48,51] The solid and total displacements are imposed and equal at $x=-d$ and vanish at the rigid boundary $x=0$. They can be written using trigonometric functions as

$$u^s = (A_1 \sin(k_1 x) + A_2 \sin(k_2 x) + B_1 \cos(k_1 x) + B_2 \cos(k_2 x))e^{j\omega t}, \tag{22}$$

$$u^t = (\mu_1 A_1 \sin(k_1 x) + \mu_2 A_2 \sin(k_2 x) + \mu_1 B_1 \cos(k_1 x) + \mu_1 B_2 \cos(k_2 x))e^{j\omega t}. \tag{23}$$

Both displacements are zero at $x=0$ and $B_1=B_2=0$. At $x=-d$,

$$u_0 = -A_1 \sin(k_1 d) - A_2 \sin(k_2 d), \tag{24}$$

$$u_0 = -\mu_1 A_1 \sin(k_1 d) - \mu_2 A_2 \sin(k_2 d), \tag{25}$$

which leads to

$$A_1 = \frac{(\mu_2 - 1)u_0}{(\mu_1 - \mu_2)\sin(k_1 d)}, \quad A_2 = \frac{(\mu_1 - 1)u_0}{(\mu_2 - \mu_1)\sin(k_2 d)}. \tag{26}$$

Note that the solid and total displacements can be written with Eq. (14) representation as

$$u_1' = \frac{A_1}{2i} = -u_1, \quad u_2' = \frac{A_2}{2i} = -u_2. \tag{27}$$

The particular solution can be obtained with the method in Appendix A. The general solution corresponds to a zero nonlinear displacement at $x=-d$ and $x=0$, and its amplitudes are solutions of the system

$$\begin{bmatrix} 1 & 1 & 1 & 1 \\ \ddot{\mu}_1 & \ddot{\mu}_2 & \ddot{\mu}_1 & \ddot{\mu}_2 \\ e_1 & e_2 & e_1' & e_2' \\ \ddot{\mu}_1 e_1 & \ddot{\mu}_2 e_2 & \ddot{\mu}_1 e_1' & \ddot{\mu}_2 e_2' \end{bmatrix} \begin{Bmatrix} \gamma_1 \\ \gamma_2 \\ \gamma_1' \\ \gamma_2' \end{Bmatrix} = \begin{Bmatrix} \sum_{i=1}^{4} \alpha_i + \alpha_i' \\ \sum_{i=1}^{4} \beta_i + \beta_i' \\ \sum_{i=1}^{4} \alpha_i e^{2jk_i d} + \alpha_i' e^{-2jk_i d} \\ \sum_{i=1}^{4} \beta_i e^{2jk_i d} + \beta_i' e^{-2jk_i d} \end{Bmatrix}. \tag{28}$$

It is straightforward to find numerical values of the amplitudes γ_i using Cramer's method.

In Fig. 3, the stress magnitude at $x=0$ for a slab of 10 cm thickness is plotted as a function of frequency. The main difference compared to the semi-infinite case is the presence of resonances both for the linear fluid pressure p_l and the solid stress σ_l^s, originating from the limited size of the slab. The first resonance of the total stress σ_l^t occurs at frequency of 1 kHz, which corresponds to the longitudinal velocity in the solid frame over twice the slab thickness. The higher

resonance frequencies are almost multiple of the first resonance frequency but not exactly due to the velocity dispersion (see the zoom in the low-frequency region in the inset). Due to the increasing attenuation with frequency in the solid frame, these resonances have decreasing maximum values with increasing frequency. For the linear fluid pressure p_l, some resonances also occur, but due to the higher contribution of the solid stress compared to the fluid pressure at these low frequencies, there is a competition between the resonances associated with the equivalent fluid slab and the resonances corresponding to the solid frame slab. This results in asymmetric resonance curves, with lower quality factors than for the solid stress. The other features of these transmitted stresses through a slab of porous medium are comparable to the semi-infinite case in Fig. 1. Note that close to the resonance frequencies, for which the stress magnitudes are higher than in the semi-infinite case, the assumptions of the developed theory could be locally violated. One should notice that these results are in qualitative agreement with experimental results obtained in the same configuration in the context of acoustic probing of the granular compaction process.[48,51] First, the acoustic transfer function between two transducers placed on opposite sides of the granular container (the present granular slab) has the same shape as the total stress σ_l^t, including the local minimum observed at the crossover for the characteristic frequency f_c. The compaction process, which consists in applying vertical discrete vibrations to a cell containing a packing of beads in order to reduce its volume, modifies strongly the solid frame elastic properties but only slightly for the geometrical properties (few %). What is observed along a compaction process is a strong increase in the acoustic transfer function magnitude of the medium slab for the frequencies lower than f_c, corresponding to a region where the solid stress dominates over the fluid pressure, while the acoustic transfer function amplitude for frequencies higher than f_c slightly diminishes. In this higher-frequency region, the fluid pressure dominates over the solid stress, and the decrease in the acoustic transfer function magnitude is explained by the few % change in the geometrical properties of the packing.

Considering the nonlinear contributions, we remind that the frequency axis corresponds to the fundamental frequency at ω; therefore, the nonlinear magnitude plotted at frequency of 5 kHz, for instance, corresponds to the one of the second harmonic at 10 kHz. In this respect, the observed resonances for the nonlinear stresses are located roughly at each 500 Hz, at least for the first ones, with differences in their magnitudes (see the inset in Fig. 3). There is actually a difference when both the fundamental wave at frequency ω is at a resonance and the second harmonic wave at 2ω is also at a resonance compared to the case where only the wave at 2ω is at a resonance of the slab. When the fundamental wave is at a resonance of the slab, the nonlinear source term in Eq. (12) is also at a local maximum in frequency, and the second harmonic wave is efficiently generated. Moreover, due to the almost regularly spaced resonances, the second harmonic wave is itself at a resonance of the slab. This results in a strong resonance for the second harmonic wave, such as frequencies of 1, 2, and 3 kHz. When the second harmonic wave is at a resonance of the slab but not the fundamental wave, the nonlinear source term is not maximum and the second harmonic is less efficiently generated; being at a resonance of the slab, it still exhibits a resonance (fundamental frequencies of 500 Hz, 1.5 kHz, and 2.5 kHz, for instance) but smaller than in the previous case.

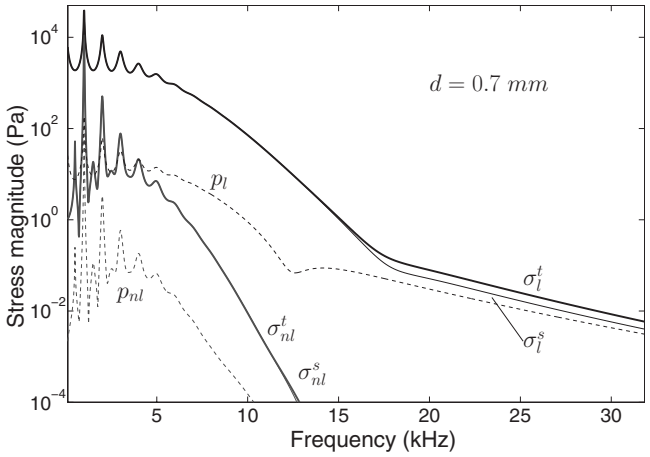

FIG. 4. Stress magnitude at $x=0$ for the same conditions as in Fig. 3, except that the bead diameter is decreased down to $d=0.7$ mm.

IV. INFLUENCE OF SOME MEDIUM PARAMETERS

In this section, the influence of three medium parameters on the previous results is analyzed: the bead diameter, the fluid properties, and the static stress applied on the granular solid frame, with the fluid static pressure being kept the same.

A. Influence of the bead diameter

The role of the bead diameter on the previous results is difficult to understand completely. To the authors' knowledge, the relation between the bead size and the acoustic energy dissipation in the solid frame is not yet understood. In addition, the relation between the bead size and the velocity dispersion in three-dimensional disordered granular media is not straightforward. However, the bead diameter role on the other parameters of the Biot model is quite well understood in the literature and follows the scaling laws given in Appendix B. Consequently, we choose to keep the same attenuation law in the solid frame and to scale the velocity dispersion law according to its chosen expression for this article, which depends on the bead diameter (see Appendix B). The nonlinear quadratic parameter D is considered independent of the bead diameter. Considering the current lack of understanding on this aspect, the possible dependence on the bead diameter is beyond the scope of the present article. In the assumptions of the developed model, a modification of D would have the only effect to shift up or down the nonlinear stress magnitudes proportional to D.

In Fig. 4, the stress magnitude at $x=0$ is plotted for the slab configuration as in Fig. 3 for a bead diameter $d=0.7$ mm. The main effect of decreasing the bead diameter is observed on the frequency region where the fluid pressure rules the total stress behavior, i.e., above the characteristic

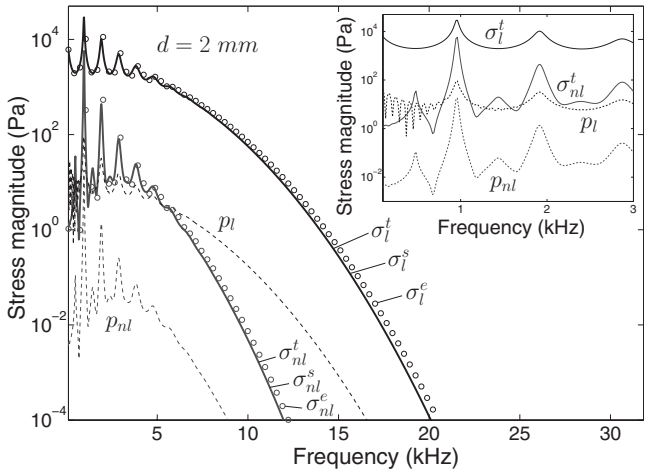

FIG. 5. Stress magnitudes in the same configuration as in Fig. 3 except that the saturating fluid is water. The inset is a zoom of the low-frequency region, showing oscillations of the fluid pressure magnitude.

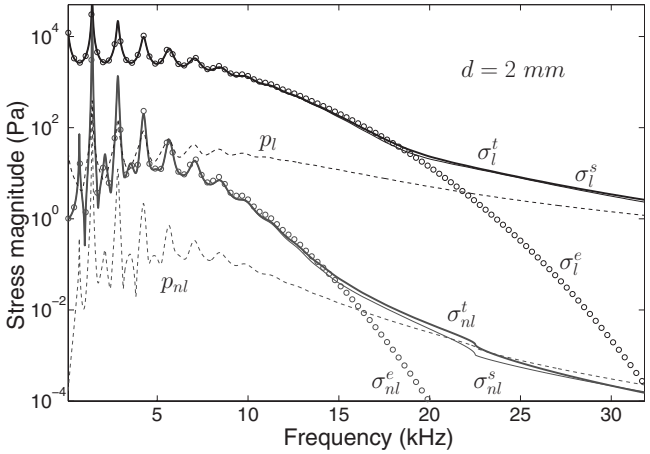

FIG. 6. Stress magnitudes in the same configuration as in Fig. 3 except that the elastic properties of the solid frame are modified due to the application of a stronger static solid stress (100 kPa).

frequency f_c. Note that in this region, in contrast to Fig. 3, the solid stress still dominates over the fluid pressure. The resistivity $\sigma \sim d^{-2}$ is increased by one order of magnitude when d is changed from 2 to 0.7 mm (see Appendix B) and the characteristic lengths decrease. This ensures a stronger attenuation of the acoustic energy in the fluid. This is clearly visible when comparing the solid and total stress magnitudes in Figs. 3 and 4 above the characteristic frequency. This behavior has also been confirmed in experiments.[48] For the second harmonic generation, the same remarks apply.

B. Influence of the saturating fluid properties

In order to modify the fluid properties and to stay in a realistic situation from the point of view of the possible experiments, we change the air considered previously for water. We neglect the possible effects of water on the solid frame properties, including the possible lubrication at the contacts, and the consequently modified attenuation law inside the solid frame.

In this case, the main difference is associated with the appearance of a strong asynchronism between the wave velocity in the equivalent fluid, close to that of water ($\sim$1500 m/s), and the much lower wave velocity in the solid frame ($\sim$200 m/s). This was not the case for air where both velocities were comparable.

The consequence is the occurrence of oscillations in the fluid pressure magnitude as a function of frequency in the low-frequency region of the presented results (see the inset in Fig. 5). These oscillations are visible here due to the better coupling between the solid frame and the fluid than in Fig. 3 for air, and the characteristic distance between two successive minima is well explained by the difference in the two wave numbers k_1 and k_2.

Another feature related to the saturating fluid properties is associated with the efficient coupling between water and the granular solid frame. In contrast to Fig. 3, there is no crossover between a region ruled by the solid stress behavior and a region ruled by the fluid pressure behavior as a function of frequency. Due to the stronger coupling, the attenuation in the solid frame (the one observed for the elastic stress σ_l^e) rules the attenuation of the fluid pressure too. Consequently, the solid stress dominates the fluid pressure in magnitude for the whole frequency range in Fig. 5 and is close to the elastic stress. This observation should be checked carefully in experiments in the future because it is in contradiction with the idea that for water-saturated granular media, most of the acoustic energy propagates through water.

C. Influence of the static solid stress

In several existing experimental results, a static stress of the order of 100 kPa is applied on the granular slab.[19,13,14] In this case, while the geometrical properties of the packing are almost not modified, the elastic properties of the solid frame are strongly different. The acoustic attenuation decreases both due to decreasing dissipation and decreasing scattering, and the wave velocity increases with some power law, mainly due to the nonlinearity of the contacts.[18,19,7,14] Consequently, in order to take into account an increase in the applied static stress on the solid frame properties, we keep constant the geometrical properties and modify only the real and imaginary parts of the elastic modulus λ_c for the solid frame. We choose $\Re e(\lambda_c)$ two times larger than previously mentioned (corresponding roughly to an increase of one order of magnitude of the applied static stress) and a two times smaller $\Im m(\lambda_c)$. Each parameter is identical to that used in Fig. 3. Results are given in Fig. 6. The main effect of increasing the static solid stress is to shift to higher frequencies the occurrence of the crossover between the frequency regions ruled by the solid stress and the fluid pressure behaviors. It means that the higher the static solid stress is, the wider the frequency region dominated by the solid stress is. This effect has been confirmed by recent experiments.[48,51]

V. CONCLUSIONS

An extension of the Biot theory for nonlinear propagation in unconsolidated model granular media or more generally in porous media supporting Biot waves is presented. The method of successive approximations is used to determine

the nonlinear solutions for the particular case of a quadratic nonlinearity of the solid. Both linear and second harmonic results can be used in future investigations on the acoustics of granular media. In particular, it has been shown that there exists a crossover frequency between a solid-controlled and a fluid-controlled behavior. This result can guide future experiments on the probing of the acoustical properties of granular packings, especially in the context where the linear or nonlinear elastic properties of the solid frame are studied. The influence of some medium parameters (bead diameter, saturating fluid, and application of a static solid stress) has also been studied.

Future works among which some are currently in progress concern the study of the nonlinear self-demodulation process or difference frequency generation, the self-action process, and the consideration of other types of nonlinearities in the solid or in the fluid. The application of the developed approach to other porous media including polymer foams, trabecular bone,[46] or other media supporting Biot waves is in principle possible.

ACKNOWLEDGMENTS

We would like to thank D. Lafarge, V. Gusev, and J.-F. Allard for stimulating discussions. This work has been supported by ANR project "grANuLar" under Grant No. NT05-3_41989.

APPENDIX A: PARTICULAR SOLUTION

This appendix presents a method to calculate the particular solution of Eq. (12) in the one-dimensional case.

1. Case of the porous media

The spatial derivatives of the solid displacement field [Eq. (14)] are

$$\frac{\partial u_l}{\partial x} = -jk_1u_1e^{-jk_1x} - jk_2u_2e^{-jk_2x} + jk_1u_1'e^{jk_1x} + jk_2u_2'e^{jk_2x}, \tag{A1a}$$

$$\frac{\partial^2 u_l}{\partial x^2} = -k_1^2u_1e^{-jk_1x} - k_2^2u_2e^{-jk_2x} - k_1^2u_1'e^{jk_1x} - k_2^2u_2'e^{jk_2x}. \tag{A1b}$$

Hence, with $2k_3=k_1+k_2$ and $2k_4=k_1-k_2$,

$$\begin{aligned}\frac{\partial u_l}{\partial x}\frac{\partial^2 u_l}{\partial x^2} = {} & jk_1^3u_1^2e^{-2jk_1x} - jk_1^3u_1'^2e^{2jk_1x} + jk_2^3u_2^2e^{-2jk_2x} \\ & - jk_2^3u_2'^2e^{2jk_2x} + 2jk_1k_2k_3u_1u_2e^{-2jk_3x} \\ & - 2jk_1k_2k_3u_1'u_2'e^{2jk_3x} - 2jk_1k_2k_4u_1'u_2e^{-2jk_4x} \\ & + 2jk_1k_2k_4u_2'u_1e^{2jk_4x}.\end{aligned} \tag{A2}$$

The particular solution reads as

$$u_p^s = \alpha_0 + \sum_{i=1}^{8} \alpha_i e^{-2jk_ix}, \tag{A3}$$

$$u_p^t = \beta_0 + \sum_{i=1}^{8} \beta_i e^{-2jk_ix}. \tag{A4}$$

For $i>4$, $k_i=-k_{i-4}$, $\alpha_i=\alpha_i'$, and $\beta_i=\beta_i'$. As the product [Eq. (A2)] does not involve constant terms, one has

$$\ddot{\rho}_s\alpha_0 + \tilde{\gamma}\ddot{\rho}_E\beta_0 = 0, \quad \ddot{\gamma}\tilde{\rho}_{\mathrm{eq}}\alpha_0 + \ddot{\rho}_{\mathrm{eq}}\beta_0 = 0, \tag{A5}$$

and thereby $\alpha_0=\beta_0=0$. The other amplitudes are the solutions of the following system:

$$\begin{bmatrix} 4\omega^2\ddot{\rho}_s[\mathbf{I}_8] - 4\lambda_c[\mathbf{k}]^2 & 4\omega^2\ddot{\gamma}\ddot{\rho}_{\mathrm{eq}}[\mathbf{I}_8] \\ 4\omega^2\ddot{\gamma}\ddot{\rho}_{\mathrm{eq}}[\mathbf{I}_8] & 4\omega^2\ddot{\rho}_{\mathrm{eq}}[\mathbf{I}_8] - 4\ddot{K}_{\mathrm{eq}}[\mathbf{k}]^2 \end{bmatrix} \begin{Bmatrix} \boldsymbol{\alpha} \\ \boldsymbol{\alpha}' \\ \boldsymbol{\beta} \\ \boldsymbol{\beta}' \end{Bmatrix} = \begin{Bmatrix} \boldsymbol{\nu} \\ \mathbf{0}_8 \end{Bmatrix}, \tag{A6}$$

where $[\mathbf{k}]$ is the diagonal matrix of the k_i wave numbers and $\boldsymbol{\nu}$ is defined by

$$\begin{aligned}\boldsymbol{\nu} = j\{ & k_1^3u_1^2, k_2^3u_2^2, 2k_1k_2k_3u_1u_2, -2k_1k_2k_4u_1'u_2, -k_1^3u_1'^2, \\ & -k_2^3u_2'^2, -2k_1k_2k_3u_1'u_2', 2k_1k_2k_4u_2'u_1\}^t.\end{aligned} \tag{A7}$$

It is possible to find analytical expressions of the solutions

$$\alpha_i = \frac{\nu_i}{4\omega^2\ddot{\rho}_{\mathrm{eq}} - 4\lambda_c k_i^2 - \dfrac{4\omega^2\ddot{\gamma}\ddot{\rho}_{\mathrm{eq}}}{4\omega^2\ddot{\rho}_{\mathrm{eq}} - 4\ddot{K}_{\mathrm{eq}}k_i^2}}, \tag{A8}$$

$$\beta_i = -\frac{4\omega^2\ddot{\gamma}\ddot{\rho}_{\mathrm{eq}}}{4\omega^2\ddot{\rho}_{\mathrm{eq}} - 4\ddot{K}_{\mathrm{eq}}k_i^2}\alpha_i. \tag{A9}$$

2. Case of the pure elastic solid

In the case of a pure elastic solid, the linear elastic displacement is

$$u_l^e = u_fe^{-jk_0x} + u_f'e^{jk_0x}, \tag{A10}$$

with $k_0=\omega\sqrt{\tilde{\rho}/\lambda_c}$. The partial derivatives of the displacement [Eq. (A10)] are

$$\frac{\partial u_l^e}{\partial x} = -jk_0u_fe^{-jk_0x} + jk_0u_f'e^{jk_0x}, \tag{A11a}$$

$$\frac{\partial^2 u_l^e}{\partial x^2} = -k_0^2u_fe^{-jk_0x} - k_0^2u_f'e^{jk_0x}, \tag{A11b}$$

where k_0 corresponds to the wave number of the compressional waves and

$$\frac{\partial u_l}{\partial x}\frac{\partial^2 u_l}{\partial x^2} = jk_0^3u_f^2e^{-2jk_0x} - jk_0^3u_f'^2e^{2jk_0x}. \tag{A12}$$

The particular solution is

$$u_p^s = \alpha_0e^{-2jk_0x} + \alpha_0'e^{2jk_0x}, \tag{A13}$$

where α_0 and α_0' are solutions of

$$(4\omega^2\rho_0 - 4\lambda_c k_0^2)(\alpha_0 e^{-2jk_0x} + \alpha_0' e^{2jk_0x}) = \alpha j k_0^3 u_f^2 e^{-2jk_0x} - jk_0^3 u_f'^2 e^{2jk_0x}. \quad \text{(A14)}$$

Finally, we obtain

$$\alpha_0 = \frac{\alpha j k_0^3 u_f^2}{4\omega^2\rho_0 - 4\lambda_c k_0^2}, \quad \text{(A15)}$$

$$\alpha_0' = -\frac{\alpha j k_0^3 u_f'^2}{4\omega^2\rho_0 - 4\lambda_c k_0^2}. \quad \text{(A16)}$$

APPENDIX B: PARAMETERS OF THE MODEL

This appendix provides the expressions of the inertial and constitutive parameters of the model for a circular frequency ω. The geometrical and physical parameters of the equivalent fluid model have been derived previously in the literature for air saturating disordered packings of solid spheres.[21] In the general case they depend on the fluid properties and on the bead diameter.

The density terms are

$$\rho_1 = (1-\phi)\rho_s, \quad \rho_2 = \phi\rho_0, \quad \rho_{12} = -\phi\rho_0(\alpha_\infty - 1), \quad \text{(B1)}$$

where ϕ is the porosity, ρ_s is the frame material density, ρ_0 is the interstitial fluid density, and α_∞ is the geometric tortuosity. ρ_{12} accounts for the interaction between the inertia forces of the solid and fluid phases. The apparent coupling density can be introduced in the form

$$\tilde{\rho}_{12} = \rho_{12} - \frac{\tilde{b}}{j\omega}.$$

The viscous effects are modeled through the following coefficient:

$$\tilde{b} = j\omega\phi\rho_0(\tilde{\alpha} - \alpha_\infty), \quad \text{(B2)}$$

where $\tilde{\alpha}$ is the dynamic tortuosity defined by

$$\tilde{\alpha} = 1 - \frac{j\phi\sigma}{\alpha_\infty\rho_0\omega}\sqrt{1 - \frac{4j\alpha_\infty^2\eta_a\rho_0\omega}{(\sigma\Lambda\phi)^2}}. \quad \text{(B3)}$$

Here, σ is the flow resistivity, η_a is the dynamic viscosity of the saturating fluid, and Λ is the viscous characteristic length. The equivalent density $\tilde{\rho}_{\mathrm{eq}}$ and the coupling coefficient $\tilde{\gamma}$ are then given by

$$\tilde{\rho}_{\mathrm{eq}} = \frac{\rho_0\tilde{\alpha}}{\phi^2}, \quad \tilde{\gamma} = \phi\left(\frac{\tilde{\rho}_{12}}{\rho_0\tilde{\alpha}} - \frac{1-\phi}{\phi}\right). \quad \text{(B4)}$$

The thermal effects are introduced through the dynamic compressibility

$$K_f = \frac{\phi\gamma P_0}{\gamma - (\gamma-1)\left[1 + \frac{8\eta_a}{j\Lambda'\mathrm{Pr}\omega\rho_0}\sqrt{1 + \frac{j\rho_0\omega\mathrm{Pr}\Lambda'^2}{16\eta_a}}\right]^{-1}}, \quad \text{(B5)}$$

where Λ' is the thermal characteristic length, Pr is the Prandtl number, P_0 is the ambient pressure, and γ is the specific heat ratio of the fluid.

The compressibility of the fluid M is then obtained as

$$M = \frac{K_r^2}{K_r(1 + \phi K_r/(K_f - 1)) - K_s}. \quad \text{(B6)}$$

The porosity ϕ of the medium can be evaluated for random close packings of spheres[3] as $\phi \simeq 0.4 \pm 0.04$. The tortuosity for disordered packings of beads is evaluated as $\alpha_\infty = 1.36$ and is independent of the bead diameter. The thermal characteristic length reads as $\Lambda' = \phi d/3(1-\phi)$. The viscous characteristic length is estimated as $\Lambda \simeq \Lambda'/3$. The flow resistivity is $\sigma = 4\eta_a F/\Lambda^2$, where $F = 3.4$ is a formation factor independent of the bead diameter.

In summary, the bead size scaling laws for the equivalent fluid parameters are $\alpha_\infty \sim \phi \sim F \sim d^0$, $\Lambda \sim \Lambda' \sim d^1$, and $\sigma \sim d^{-2}$.

Concerning the parameters of the solid frame, they are much less characterized and can vary by several orders of magnitude depending on the applied external conditions and the state of the packing. They have been chosen here to correspond to the experimental conditions of some available experimental results,[48,51] i.e., a weak external static stress of ~ 3 kPa, giving a measured wave velocity of ~ 200 m/s at low frequencies. Due to the existing velocity dispersion in experiments, we considered an elastic modulus for the solid frame of the form $\lambda_c = \lambda_{c0}[(\omega/\omega_c)/\arcsin(\omega/\omega_c)]^2 + i\xi\lambda_{c0}\omega$. The real part corresponds to the dispersion relation of a one-dimensional granular chain[52] with $\omega_c = d/2\sqrt{\lambda_{c0}/\rho_s}$, $\lambda_{c0} = 60$ MPa, and $\rho_s = 1500$ kg/m^3. The imaginary part is chosen to be proportional to the frequency in order to increase with frequency. Another dependency can in principle be chosen. A value of $\xi = 4 \times 10^{-6}$ provides an attenuation close to the one observed in experiments.[48,51] Note that these dispersion and attenuation laws may not fulfill the Kramers–Kronig relations and this could provide causality problems if the results obtained in the frequency domain in this article are transformed into the time domain.

The two compressional waves of the porous medium are defined by their wave number k_i and the ratio μ_i of the total displacement over the solid one. They are defined by

$$k_i^2 = \frac{(\delta_{s2}^2 + \delta_{\mathrm{eq}}^2) \pm \sqrt{(\delta_{s2}^2 + \delta_{\mathrm{eq}}^2)^2 - 4\delta_{\mathrm{eq}}^2\delta_{s1}^2}}{2}, \quad \text{(B7)}$$

with

$$\delta_{\mathrm{eq}} = \omega\sqrt{\frac{\tilde{\rho}_{\mathrm{eq}}}{M}}, \quad \delta_{s1} = \omega\sqrt{\frac{\tilde{\rho}}{\lambda_c}}, \quad \delta_{s2} = \omega\sqrt{\frac{\tilde{\rho}_s}{\lambda_c}}, \quad \text{(B8)}$$

where

$$\tilde{\rho} = \rho_1 - \tilde{\rho}_{12} - \frac{\tilde{\rho}_{12}^2}{\rho_2 - \tilde{\rho}_{12}}, \quad \tilde{\rho}_s = \tilde{\rho} + \tilde{\gamma}^2\tilde{\rho}_{\mathrm{eq}}, \quad \text{(B9)}$$

$$\mu_i = \tilde{\gamma}\frac{(k_i^2 - \delta_{s2}^2)}{\delta_{s2}^2 - \delta_{s1}^2} = \tilde{\gamma}\frac{\delta_{\mathrm{eq}}^2}{k_i^2 - \delta_{\mathrm{eq}}^2}. \quad \text{(B10)}$$

[1] P. G. de Gennes, "Granular matter: A tentative view," Rev. Mod. Phys. **71**, S374–S382 (1999).
[2] H. M. Jaeger and S. R. Nagel, "Physics of the granular state," Science **255**, 1523–1531 (1992).

[3]P. Richard, M. Nicodemi, R. Delannay, P. Ribière, and D. Bideau, "Slow relaxation and compaction of granular systems," Nature Mater. **4**, 121–128 (2005).
[4]H. A. Makse, N. Gland, D. L. Johnson, and L. Schwartz, "Granular packings: Nonlinear elasticity, sound propagation, and collective relaxation dynamics," Phys. Rev. E **70**, 061302 (2004).
[5]N. Xu, N. Wyart, A. J. Liu, and S. R. Nagel, "Excess vibrational modes and the boson peak in model glasses," Phys. Rev. Lett. **98**, 175502 (2007).
[6]C. S. O'Hern, L. E. Silbert, A. J. Liu, and S. R. Nagel, "Jamming at zero temperature and zero applied stress: The epitome of disorder," Phys. Rev. E **68**, 011306 (2003).
[7]K. L. Johnson, *Contact Mechanics* (Cambridge University Press, Cambridge, 1985).
[8]R. D. Mindlin and H. Deresiewicz, "Elastic spheres in contact under varying oblique forces," J. Appl. Mech. **21**, 327–344 (1953).
[9]I. Y. Belyaeva, V. Y. Zaitsev, and E. M. Timanin, "Experimental study of nonlinear elastic properties of granular media with nonideal packing," Sov. Phys. Acoust. **40**, 789–793 (1994).
[10]P. A. Johnson and X. Jia, "Nonlinear dynamics, granular media and dynamic earthquake triggering," Nature (London) **437**, 871–874 (2005).
[11]V. Tournat, B. Castagnède, V. E. Gusev, and Ph. Béquin, "Self-demodulation acoustic signatures for non-linear propagation in glass beads," C. R. Mec. **331**, 119–125 (2003).
[12]V. Tournat, V. E. Gusev, and B. Castagnède, "Subharmonics and noise excitation in transmission of acoustic wave through unconsolidated granular medium," Phys. Lett. A **326**, 340–348 (2004).
[13]V. Tournat, V. E. Gusev, V. Yu. Zaitsev, and B. Castagnède, "Acoustic second harmonic generation with shear to longitudinal mode conversion in granular media," Europhys. Lett. **66**, 798–804 (2004).
[14]V. Tournat, V. Yu. Zaitsev, V. E. Gusev, V. E. Nazarov, P. Béquin, and B. Castagnède, "Probing weak forces in granular media through nonlinear dynamic dilatancy: Clapping contacts and polarization anisotropy," Phys. Rev. Lett. **92**, 085502 (2004).
[15]V. Tournat, V. Yu. Zaitsev, V. E. Nazarov, V. E. Gusev, and B. Castagnède, "Experimental study of nonlinear acoustic effects in a granular medium," Acoust. Phys. **51**, 543–553 (2005).
[16]V. Yu. Zaitsev, V. E. Nazarov, V. Tournat, V. Gusev, and B. Castagnède, "Luxembourg-Gorky effect in a granular medium: Probing perturbations of the material state via cross-modulation of elastic waves," Europhys. Lett. **70**, 607–613 (2005).
[17]D. M. Mueth, H. M. Jaeger, and S. R. Nagel, "Force distribution in a granular medium," Phys. Rev. E **57**, 3164–3169 (1998).
[18]J. D. Goddard, "Nonlinear elasticity and pressure-dependent wave speeds in granular media," Proc. R. Soc. London, Ser. A **430**, 105–131 (1990).
[19]X. Jia, C. Caroli, and B. Velicky, "Ultrasound propagation in externally stressed granular media," Phys. Rev. Lett. **82**, 1863–1866 (1999).
[20]C. Josserand, A. V. Tkachenko, D. M. Mueth, and H. M. Jaeger, "Memory effects in granular materials," Phys. Rev. Lett. **85**, 3632–3635 (2000).
[21]J.-F. Allard, M. Henry, J. Tizianel, L. Kelders, and W. Lauriks, "Sound propagation in air-saturated random packings of beads," J. Acoust. Soc. Am. **104**, 2004–2007 (1998).
[22]K. V. Horoshenkov and J. Swift, "The acoustic properties of granular materials with pore size distribution close to log-normal," J. Acoust. Soc. Am. **110**, 2371–2378 (2001).
[23]G. Pispola, K. V. Horoshenkov, and F. Asdrubali, "Transmission loss measurement of consolidated granular media," J. Acoust. Soc. Am. **117**, 2716–2719 (2005).
[24]K. Attenborough, "Models for the acoustical characteristics of air filled granular materials," Acta Acust. **1**, 213–226 (1993).
[25]O. Umnova, K. Attenborough, and K. M. Li, "A cell model for the acoustical properties of packings of spheres," J. Acoust. Soc. Am. **87**, 226–235 (2001).
[26]O. Umnova, K. Attenborough, H.-C. Shin, and A. Cummings, "Response of multiple rigid porous layers to high levels of continuous acoustic excitation," J. Acoust. Soc. Am. **116**, 703–712 (2004).
[27]C. Ayrault and S. Griffiths, "Separation of viscothermal losses and scattering in ultrasonic characterization of porous media," Ultrasonics **45**, 40–49 (2006).
[28]H. P. Schriemer, M. L. Cowan, J. H. Page, P. Sheng, Z. Liu, and D. A. Weitz, "Energy velocity of diffusing waves in strongly scattering media," Phys. Rev. Lett. **79**, 3166–3169 (1997).
[29]A. Moussatov, B. Castagnède, and V. Gusev, "Observation of nonlinear interaction of acoustic waves in granular materials: Demodulation process," Phys. Lett. A **283**, 216–223 (2001).
[30]M. Biot, "Mechanics of deformation and acoustic propagation in porous media," J. Appl. Phys. **33**, 1482–1498 (1962).
[31]M. A. Biot, "Theory of propagation of elastic waves in a fluid-filled-saturated porous solid," J. Acoust. Soc. Am. **28**, 168–191 (1956).
[32]J. G. Berryman, "Confirmation of Biot's theory," Appl. Phys. Lett. **37**, 382–384 (1980).
[33]T. J. Plona, "Observation of a second bulk compressional wave in a porous medium at ultrasonic frequencies," Appl. Phys. Lett. **36**, 259–261 (1980).
[34]J. L. Auriault, L. Borne, and R. Chambon, "Dynamics of porous saturated media, checking of the generalized law of Darcy," J. Acoust. Soc. Am. **77**, 1641–1650 (1985).
[35]R. Burridge and J. B. Keller, "Poroelasticity equations derived from microstructure," J. Acoust. Soc. Am. **70**, 1140–1146 (1981).
[36]S. R. Pride and J. G. Berryman, "Connecting theory to experiments in poroelasticity," J. Mech. Phys. Solids **46**, 719–747 (1998).
[37]S. R. Pride, A. F. Gangi, and F. D. Morgan, "Deriving the equations of motion for porous isotropic media," J. Acoust. Soc. Am. **92**, 3278–3290 (1992).
[38]J. F. Allard, *Propagation of Sound in Porous Media, Modelling Sound Absorbing Materials* (Elsevier Applied Science, London and New York, 1993).
[39]Y. Champoux and J. F. Allard, "Dynamic tortuosity and bulk modulus in air-saturated porous media," J. Appl. Phys. **70**, 1975–1979 (1991).
[40]D. L. Johnson, J. Koplik, and R. Dashen, "Theory of dynamic permeability and tortuosity in fluid-saturated porous media," J. Fluid Mech. **176**, 379–402 (1987).
[41]D. Lafarge, P. Lemarinier, J. F. Allard, and V. Tarnow, "Dynamic compressibility of air in porous structures at audible frequencies," J. Acoust. Soc. Am. **102**, 1995–2006 (1997).
[42]J. M. Carcione, "Wave propagation in anisotropic, saturated porous media: Plane-wave theory and numerical simulation," J. Acoust. Soc. Am. **99**, 2655–2666 (1996).
[43]O. Coussy, *Mechanics of Porous Continua* (John Wiley, New York, 1995).
[44]M. A. Biot, "Nonlinear and semilinear rheology of porous solids," J. Geophys. Res. **78**, 4924–4937 (1973).
[45]D. M. Donskoy, K. Khashanah, and T. G. McKee, Jr., "Nonlinear acoustic waves in porous media in the context of Biot's theory," J. Acoust. Soc. Am. **102**, 2521–2528 (1997).
[46]G. Renaud, S. Calle, J.-P. Remenieras, and M. Defontaine, "Exploration of trabecular bone nonlinear elasticity using time-of-flight modulation," IEEE Trans. Ultrason. Ferroelectr. Freq. Control **55**, 1497–1507 (2008).
[47]O. Dazel, B. Brouard, C. Depollier, and S. Griffiths, "An alternative Biot's displacement formulation for porous materials," J. Acoust. Soc. Am. **121**, 3509–3516 (2007).
[48]C. Inserra, "Characterization of granular compaction by linear and nonlinear acoustic methods," Ph.D. thesis, Université du Maine, Le Mans, France (2007).
[49]M. F. Hamilton and C. L. Morfey, "Model equations," in *Nonlinear Acoustics*, edited by M. F. Hamilton and D. T. Blackstock (Academic, San Diego, CA, 1998), pp. 52–56.
[50]B. K. Novikov, O. V. Rudenko, and V. I. Timoshenko, *Nonlinear Underwater Acoustics* (American Institute of Physics, New York, 1987).
[51]C. Inserra, V. Tournat, and V. E. Gusev, "Characterization of granular compaction by nonlinear acoustic resonance method," Appl. Phys. Lett. **92**, 191916 (2008).
[52]V. Tournat, V. E. Gusev, and B. Castagnède, "Self-demodulation of elastic waves in a 1D granular chain," Phys. Rev. E **70**, 056603 (2004).